2009

Proteomic analyses of native brain KV4.2 channel complexes

Celine Marionneau
Washington University School of Medicine in St. Louis

Richard D. LeDuc
Washington University School of Medicine in St. Louis

Henry W. Rohrs
Washington University School of Medicine in St. Louis

Andrew J. Link
Vanderbilt University

R. Reid Townsend
Washington University School of Medicine in St. Louis

See next page for additional authors

RESEARCH PAPER

Channels 3:4, 287-297; July/August 2009; © 2009 Landes Bioscience

Proteomic analyses of native brain $K_V4.2$ channel complexes

Céline Marionneau,[1,†] Richard D. LeDuc,[2] Henry W. Rohrs,[3] Andrew J. Link,[4] R. Reid Townsend[2,†] and Jeanne M. Nerbonne[1,*]

Departments of [1]Developmental Biology; [2]Internal Medicine and [3]Chemistry; Washington University; St. Louis, MO USA; [4]Department of Microbiology and Immunology; Vanderbilt University Medical Center; Nashville, TN USA

[†]Current address: l'institut du thorax, UMR 915; UFR de Médecine; Nantes, France

Key words: I_A, accessory subunits, mass spectrometric identification

Abbreviations: 1D-gel, one-dimensional polyacrylamide gel; 1D-LC-MS/MS, one-dimensional liquid chromatography-tandem mass spectrometry; 2D-LC-MS/MS, two-dimensional liquid chromatography-tandem mass spectrometry; DPP, dipeptidyl-peptidase; I_A, A-type voltage-gated K^+ current; IP, immunoprecipitation; KChIP, K^+ channel interacting protein; K_V α subunit, voltage-gated K^+ pore-forming (α) channel subunit; K_V β subunit, voltage-gated K^+ accessory (β) channel subunit; $K_V4.2^{-/-}$, $K_V4.2$ knock-out; MS/MS, tandem mass spectrometry; MS, mass spectrometry; MudPIT, multidimensional protein identification technology; RbIgG, rabbit immunoglobulin G; Rbα$K_V4.2$, anti-$K_V4.2$ rabbit polyclonal antibody; RIPA buffer, radioimmunoprecipitation assay buffer; WT, wild type

Somatodendritic A-type (I_A) voltage-gated K^+ (K_V) channels are key regulators of neuronal excitability, functioning to control action potential waveforms, repetitive firing and the responses to synaptic inputs. Rapidly activating and inactivating somatodendritic I_A channels are encoded by K_V4 α subunits and accumulating evidence suggests that these channels function as components of macromolecular protein complexes. Mass spectrometry (MS)-based proteomic approaches were developed and exploited here to identify potential components and regulators of native brain $K_V4.2$-encoded I_A channel complexes. Using anti-$K_V4.2$ specific antibodies, $K_V4.2$ channel complexes were immunoprecipitated from adult wild type mouse brain. Parallel control experiments were performed on brain samples isolated from ($K_V4.2^{-/-}$) mice harboring a targeted disruption of the *KCND2* ($K_V4.2$) locus. Three proteomic strategies were employed: an in-gel approach, coupled to one-dimensional liquid chromatography-tandem MS (1D-LC-MS/MS), and two in-solution approaches, followed by 1D- or 2D-LC-MS/MS. The targeted in-gel 1D-LC-MS/MS analyses demonstrated the presence of the K_V4 α subunits ($K_V4.2$, $K_V4.3$ and $K_V4.1$) and the K_V4 accessory, KChIP (KChIP1-4) and DPP (DPP6 and 10), proteins in native brain $K_V4.2$ channel complexes. The more comprehensive, in-solution approach, coupled to 2D-LC-MS/MS, also called Multidimensional Protein Identification Technology (MudPIT), revealed that additional regulatory proteins, including the K_V channel accessory subunit K_Vβ1, are also components of native brain $K_V4.2$ channel complexes. Additional biochemical and functional approaches will be required to elucidate the physiological roles of these newly identified K_V4 interacting proteins.

Introduction

Voltage-gated K^+ (K_V) channels are key regulators of neuronal excitability, functioning in the control of resting membrane potentials, action potential waveforms, repetitive firing properties, and in modulating the responses to synaptic inputs.[1-3] Molecular cloning has provided insights into the basis of neuronal K_V channel diversity with the identification of large numbers of K_V channel pore-forming (α) and accessory (β) subunits.[4] Considerable evidence suggests that functional neuronal K_V channels comprise four K_V α subunits and multiple K_V β subunits, although the role of the accessory K_V β subunits in regulating the functional expression and/or the properties of native K_V channels in neurons is poorly understood.[2-4] In addition to the primary K_V (α and β) channel subunits, accumulating evidence also suggests that K_V channels in neurons, as well as in other cell types, function as components of macromolecular complexes, containing multiple other proteins that influence channel stability, trafficking, localization and/or biophysical properties.[2,3,5,6]

Molecular genetic strategies in vivo and in vitro have revealed that neuronal A-type (I_A) currents are encoded by K_V4 α subunits and a critical role for $K_V4.2$ in the generation of somatodendritic I_A channels in cortical and hippocampal neurons has been demonstrated.[7-10] It has recently been suggested that functional brain $K_V4.2$-encoded I_A channels are ternary complexes, comprising $K_V4.2$ α subunits together with the K^+ Channel Interacting Proteins (KChIPs) and the dipeptidyl peptidase-like DPP6/DPP10 accessory proteins.[11-13] Although heterologous expression of these three ($K_V4.2$, KChIPx, DPPx) channel components recapitulates many of the properties of endogenous I_A channels,[14,15]

*Correspondence to: Jeanne M. Nerbonne; Email: jnerbonne@wustl.edu
Submitted: 05/19/09; Revised: 07/15/09; Accepted: 07/16/09
Previously published online: www.landesbioscience.com/journals/channels/article/9553

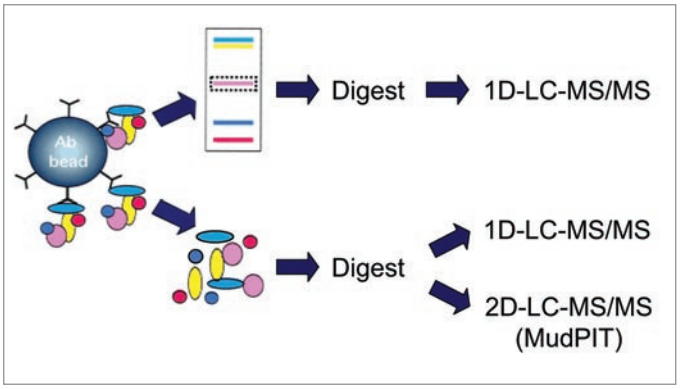

Figure 1. Schematic representation of the three distinct proteomic strategies developed to identify the components and regulators of brain $K_V4.2$ channel macromolecular protein complexes. Once eluted from the antibody-beads, the immunoprecipitated proteins are fractionated on one-dimensional polyacrylamide gels prior to in-gel digestion (top), or digested directly in-solution (bottom). The resulting tryptic peptides are identified using one- or two-dimensional liquid chromatography-tandem mass spectrometry (1D or 2D-LC-MS/MS[29,30]).

the relevance of these observations to the functioning of neuronal I_A is difficult to evaluate. Indeed, recent studies exploiting short interfering RNAs (siRNA) targeting DPP6 suggest that the functional role of DPP6 in the regulation of hippocampal I_A channels is really quite different[16] from what has been suggested based on the results of studies of channels reconstituted in heterologous cells. It seems likely, therefore, that neuronal I_A channel expression and functioning are affected by additional regulatory proteins. In addition, $K_V4.2$ channels are highly localized at synapses,[17] and considerable evidence suggests roles for $K_V4.2$-encoded I_A channels in the regulation of synaptic functioning and synaptic plasticity.[18-20]

In the experiments here, native $K_V4.2$ channel complexes were isolated from adult mouse brain, and the components of these complexes were identified by mass spectrometry (MS)-based proteomic[21-24] approaches. Different experimental strategies were exploited, and the results obtained using these different approaches are presented and compared.

Results

Proteomic strategies. Three distinct proteomic approaches were developed in parallel in efforts to identify components of native brain $K_V4.2$ channel complexes (**Fig. 1**). In each case, a polyclonal anti-$K_V4.2$ specific antibody was cross-linked to magnetic beads, and antibody-crosslinked beads were used for immunoprecipitation (IP) of $K_V4.2$ (and associated proteins) from total protein lysates prepared from adult mouse brains. Following isolation and elution of the $K_V4.2$ channel protein complexes from the antibody-crosslinked beads, two different strategies were used. In the first case, the in-gel approach, the immunoprecipitated proteins were separated on one-dimensional polyacrylamide gels (1D-gels), and selected protein bands were analyzed by one-dimensional liquid chromatography-tandem mass spectrometry (1D-LC-MS/MS). In the alternate (the in-solution) approach, the entire immunoprecipitate was digested with trypsin, and the resulting tryptic peptides were analyzed directly by mass spectrometry using either 1D- or 2D-LC-MS/MS.

Immunoprecipitation of brain $K_V4.2$ channel complexes. Initial experiments were focused on optimizing the experimental conditions for the IP of $K_V4.2$ channel protein complexes from adult wild type (WT) mouse brains. Brains from animals ($K_V4.2^{-/-}$)[10] harboring a targeted disruption in the gene (*KCND2*) encoding $K_V4.2$ were used as a control. An anti-$K_V4.2$ rabbit polyclonal antibody (Rb$\alpha K_V4.2$) was used for the IPs from WT and $K_V4.2^{-/-}$ brains, and a non-specific rabbit immunoglobulin G (RbIgG) was used in control IPs from the WT brain samples. As illustrated in **Figure 2A**, western blot analyses of the immunoprecipitated proteins probed with the monoclonal anti-$K_V4.2$ specific antibody (m$\alpha K_V4.2$) reliably revealed robust $K_V4.2$ immunoprecipitation from WT mouse brain with Rb$\alpha K_V4.2$. The immunoprecipitation of $K_V4.2$ (from WT brain) was specific as evidenced by the absence of signal in the RbIgG-IP from WT brain. No $K_V4.2$ protein was detected either in the Rb$\alpha K_V4.2$-IP from the $K_V4.2^{-/-}$ brain (**Fig. 2A**) or in the total protein lysates from the $K_V4.2^{-/-}$ brain samples (data not shown), validating the specificity of the anti-$K_V4.2$ mouse monoclonal antibody used in the western blots. Importantly, about 90% depletion of the $K_V4.2$ protein was achieved in the Rb$\alpha K_V4.2$-IP experiments as evident in the western blot analyses of $K_V4.2$ remaining in the supernatant following the IP compared with the initial sample (lower of **Fig. 2A**). These observations suggest that the isolated and analyzed proteins are representative of mouse brain $K_V4.2$ channel complexes. The immunoprecipitated proteins were then fractionated on 1D-gels and visualized using SYPRO Ruby (**Fig. 2B**). Each immunoprecipitation step was optimized to isolate $K_V4.2$ proteins in quantities sufficient for in-gel visualization and mass spectrometric identification (data not shown). Although many proteins were detected in each sample, there were a number of protein bands that were specific to the Rb$\alpha K_V4.2$-IP from WT mouse brain, i.e., they were absent in the two control IPs (**Fig. 2B**). These distinct protein bands ran at molecular weights corresponding to $K_V4.2$ (and other K_V4 α subunits) and to the previously identified K_V4 channel accessory KChIPx and DPPx subunits.[11-15] These observations suggested that the Rb$\alpha K_V4.2$-IP from WT mouse brain was enriched in the protein components of $K_V4.2$ channel complexes.

In-gel identification of $K_V4.2$ channel complex components. The SYPRO Ruby-stained protein bands, corresponding to the molecular weights of K_V4 proteins, as well as of the previously characterized K_V4 channel accessory subunits KChIPx and DPPx (**Fig. 2B**), were excised from the gels, digested in-gel with trypsin, and the resulting tryptic peptides were analyzed using 1D-LC-MS/MS. These experiments led to the reliable identification of multiple peptides derived from the $K_V4.2$ protein. A representative fragmentation spectrum of a $K_V4.2$ tryptic peptide, as well as the amino acid sequence derived from this spectrum, is illustrated in **Figure 3A**. This in-gel analysis yielded a total of seven unique $K_V4.2$ peptides, and an amino acid sequence coverage for the $K_V4.2$ protein of 14% (**Fig. 3B** and **Table 1**). In addition to the $K_V4.2$ protein, the other K_V4 α subunits ($K_V4.1$

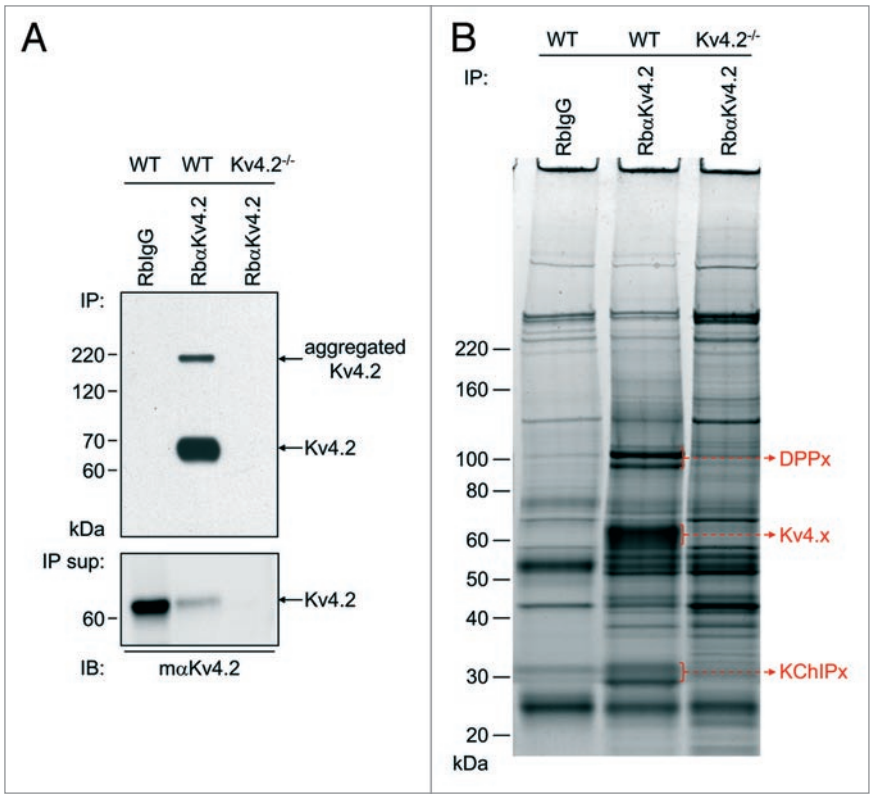

Figure 2. Immunoprecipitation of brain $K_V4.2$ channel complexes. (A) Top: representative western blot of immunoprecipitated (IP) proteins from adult WT or $K_V4.2^{-/-}$ mouse[10] brains with the anti-$K_V4.2$ rabbit polyclonal antibody (Rb$\alpha K_V4.2$) or with non-specific rabbit immunoglobulin G (RbIgG), and probed (IB) with an anti-$K_V4.2$ mouse monoclonal antibody (m$\alpha K_V4.2$). The $K_V4.2$ protein (arrow) is clearly evident in the Rb$\alpha K_V4.2$-IP from WT mouse brain, but is absent in the two control IPs; the upper band (also indicated by an arrow) corresponds to aggregated $K_V4.2$ proteins. Lower: representative western blot of the corresponding IP supernatants (IP sup) also probed with m$\alpha K_V4.2$. Analyses of these blots revealed that approximately 90% depletion of the $K_V4.2$ protein was achieved in the Rb$\alpha K_V4.2$-IP from WT brain (see text). (B) SYPRO Ruby stained-gel of immunoprecipitated samples. Proteins running at molecular weights corresponding to the $K_V4.x$ α subunits and to the previously identified K_V4 channel accessory subunits, KChIPx and DPPx,[11-15] (indicated by a red arrow) are clearly evident and have been identified using in-gel 1D-LC-MS/MS in the Rb$\alpha K_V4.2$-IP from WT mouse brain, but not in either of the control IPs.

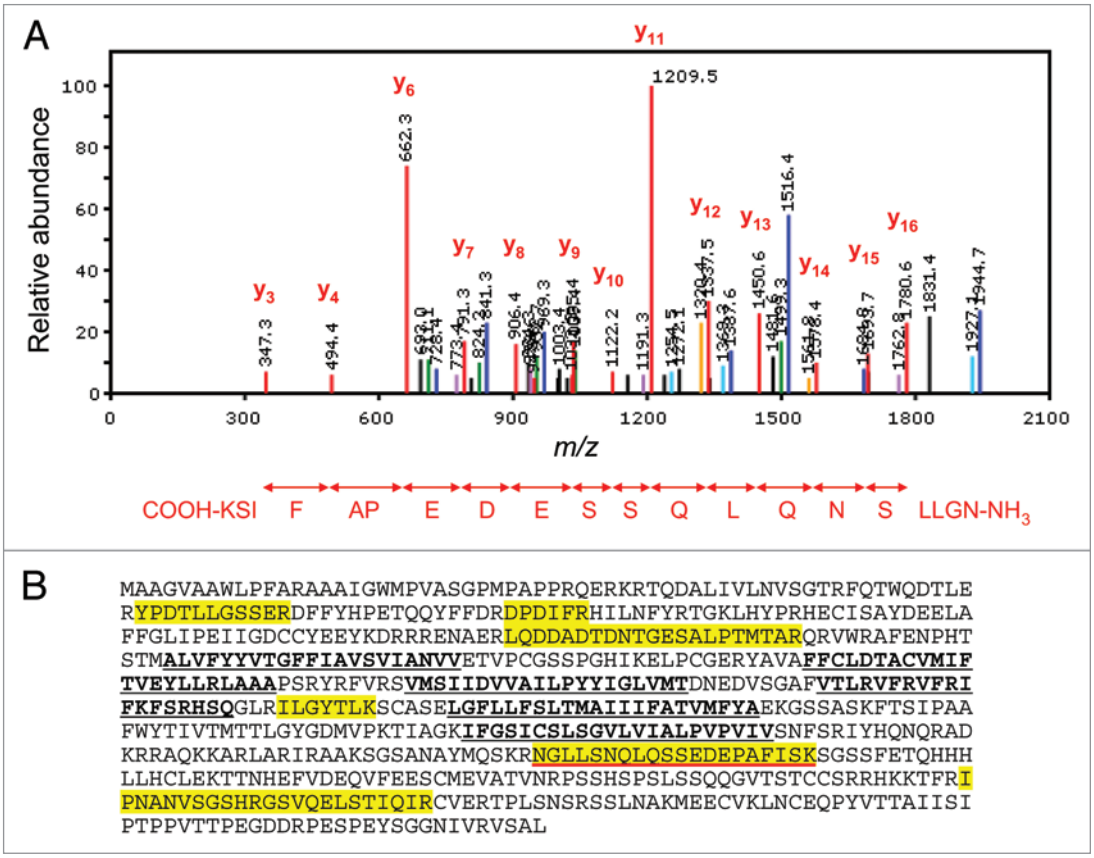

Figure 3. Mass spectrometric identification of $K_V4.2$ using in-gel digestion and 1D-LC-MS/MS. (A) Representative fragmentation spectrum of one of the identified $K_V4.2$ tryptic peptides. The signals (*m/z* values) that are consistent with doubly-charged y ions from the NH_2-NGLLSNQLQSSEDEPAFISK-COOH peptide are highlighted in red. (B) Amino acid sequence coverage obtained for the (mouse) $K_V4.2$ protein. Detected peptides are highlighted in yellow; the peptide for which the fragmentation spectrum is shown (in A) is underlined in red. Transmembrane domains are in bold and are underlined in black.

Table 1. Proteins identified in immunoprecipitated brain $K_V4.2$ channel complexes using in-gel 1D-LC-MS/MS[1]

Protein	Numbers of peptides: unique (total)	% Amino acid sequence coverage
$K_V4.2$	7 (7)	14%
$K_V4.1$	4 (4)	6%
$K_V4.3$	4 (4)	12%
KChIP1	3 (3)	14%
KChIP2	5 (6)	18%
KChIP3	5 (5)	19%
KChIP4	9 (11)	38%
DPP6	23 (28)	23%
DPP10	15 (16)	21%

[1]The numbers of unique peptides, as well as the total numbers of peptides and the percent (%) amino acid sequence coverage, for each protein are presented. Mascot protein and peptide ion scores were greater than 30, and Scaffold protein probability scores were 100% (see Suppl. Table 1). None of the proteins listed were identified in the control immunoprecipitations.

Table 2. Proteins identified in immunoprecipitated brain $K_V4.2$ channel complexes using in-solution 1D-LC-MS/MS[1]

Protein	Numbers of peptides: unique (total)	% Amino acid sequence coverage
$K_V4.2$	12 (16)	22%
$K_V4.1$	8 (9)	16%
$K_V4.3$	14 (22)	29%
KChIP1	4 (4)	18%
KChIP2	6 (8)	20%
KChIP3	5 (7)	29%
KChIP4	10 (18)	43%
DPP6	25 (29)	28%
DPP10	19 (20)	24%

[1]The numbers of unique peptides, as well as the total numbers of peptides and the percent (%) amino acid sequence coverage, for each protein are presented. Mascot protein and peptide ion scores were greater than 30, and Scaffold protein probability scores were 100% (see Suppl. Table 2). None of the proteins listed were identified in the control immunoprecipitations.

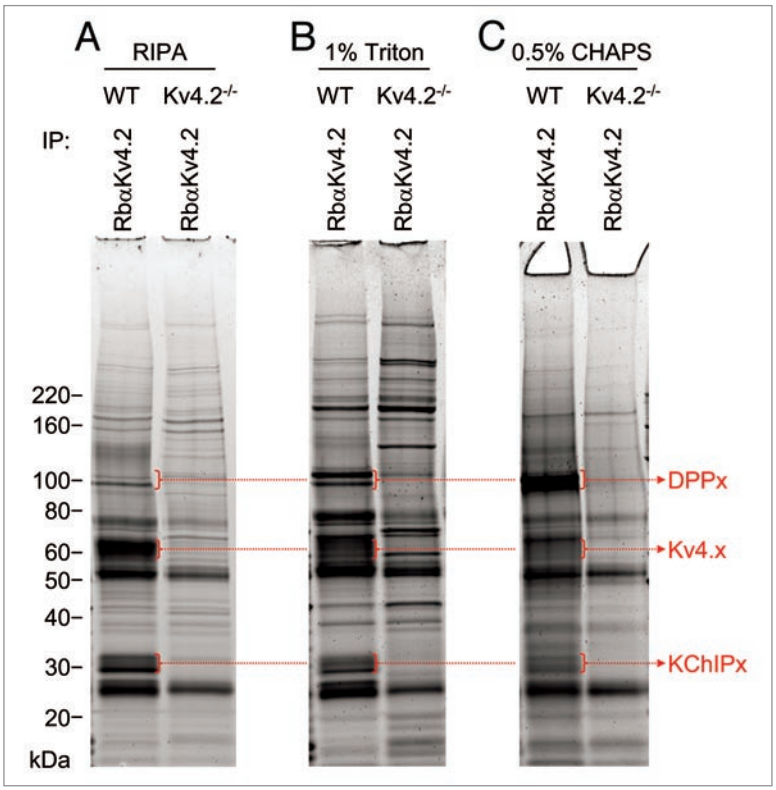

Figure 4. Comparison of detergent conditions in the isolation of brain $K_V4.2$ channel complexes. Detergents used in the solubilization and immunoprecipitation (IP) of brain $K_V4.2$ channel complexes are indicated. IP experiments were performed with the Rb$\alpha K_V4.2$ antibody from the WT and $K_V4.2^{-/-}$ brains. The relative yield of $K_V4.x$ proteins was larger in the more stringent (RIPA buffer) detergent condition (A), whereas the relative abundances of the K_V4 channel accessory subunits KChIPx and DPPx (compared with the $K_V4.x$ proteins) were greater in the less stringent (1% Triton and 0.5% CHAPS) detergent conditions (B and C).

and $K_V4.3$), as well as several previously identified K_V4 accessory subunits, KChIPs (KChIP1, KChIP2, KChIP3 and KChIP4), and DPPs (DPP6 and DPP10), were also identified. Importantly, none of these proteins were detected in the two control IPs. The numbers of unique and total peptides identified for each protein, as well as the amino acid sequence coverage obtained for each, are provided in **Table 1**. A listing of identified peptides along with the relevant scoring metrics is available in **Supplemental Table 1**.

In-solution identification of $K_V4.2$ channel complex components. To identify additional proteins immunoprecipitating with the brain $K_V4.2$ protein, the entire immunoprecipitated (i.e., without gel fractionation) protein sample was digested with trypsin, and the resulting tryptic peptides were analyzed using 1D- or 2D-LC-MS/MS. As shown in **Table 2**, the numbers of unique and total peptides detected using in-solution, as compared with in-gel, 1D-LC-MS/MS were substantially higher for $K_V4.2$ and for most of the other identified $K_V4.2$ channel accessory subunits. As a result, the amino acid sequence coverage obtained for each protein was greater. As an example, fourteen unique (and twenty-two total) $K_V4.3$ peptides were detected using in-solution 1D-LC-MS/MS (**Table 2**), as compared with four peptides using in-gel 1D-LC-MS/MS (**Table 1**). The in-solution 1D-LC-MS/MS, therefore, yielded 29% sequence coverage (**Table 2**) for the $K_V4.3$ protein compared with 12% from the in-gel 1D-LC-MS/MS method (**Table 1**). Some of the fourteen unique $K_V4.3$ peptides identified were detected several times in a single 1D-LC-MS/MS run, leading to a total of twenty-two $K_V4.3$ peptides (**Table 2**). Again, none of these peptides (and none of the peptides corresponding to the other K_V4 channel complex components) were detected in the two control IPs.

Subsequent experiments were focused on exploring directly the effects of different detergents and different solubilization and immunoprecipitation conditions on the efficiency of isolation of $K_V4.2$ channel complexes. As illustrated in **Figure 4**, the amount of immunoprecipitated $K_V4.x$ proteins was proportional to the stringency of the detergent used. Specifically, when the more stringent buffer, the RIPA buffer, was used, the amount of $K_V4.x$ proteins solubilized and isolated was high (**Fig. 4A**). However, the relative amount of the DPPx and KChIPx proteins (i.e., relative to the $K_V4.x$ proteins) was substantially greater when the less stringent 1% Triton (**Fig. 4B**) or 0.5% CHAPS (**Fig. 4C**) detergents were used. These results suggested that using less stringent detergent conditions for solubilization and immunoprecipitation was more likely to preserve channel complex protein-protein interactions, and allow the identification of novel K_V4 channel interacting and/or regulatory proteins. Interestingly, these experiments also revealed that the interactions of the DPP and the KChIP proteins with $K_V4.2$ are affected differently by the various detergents used in the solubilizations of isolated $K_V4.2$ complexes: relatively more DPP proteins were isolated in the 1% Triton (**Fig. 4B**) and 0.5% CHAPS (**Fig. 4C**) detergents, whereas relatively more KChIP proteins were obtained in the complexes isolated in the RIPA buffer (**Fig. 4A**) and in the 1% Triton (**Fig. 4B**) detergent conditions.

Using the in-solution approach does not allow direct visual comparison of the immunoprecipitated proteins. The quality of the control IPs, therefore, becomes an important point to consider before undertaking any in-solution digestion. Importantly, the preliminary experiments here revealed that the pattern of background (i.e., contaminating) proteins obtained in the two control IPs (RbIgG-IP from WT brain and Rb$\alpha K_V4.2$-IP from $K_V4.2^{-/-}$ brain) were really quite similar on SYPRO Ruby-stained gels (**Fig. 2B**). In addition, the relative abundances of the proteins in the three IPs (Rb$\alpha K_V4.2$-IP from WT brain, RbIgG-IP from WT brain and Rb$\alpha K_V4.2$-IP from $K_V4.2^{-/-}$ brain) were compared using high-resolution label-free peptide quantification. Endopeptidase digestions of each immunoprecipitate were analyzed by nano-LC-LTQ-FTICR and the peptide ion currents were aligned and quantified as described in Materials and Methods. The annotation and quantification of one of the $K_V4.2$ peptides (SGSANAYMQSK), that was detected as a doubly charged ion at m/z = 572.2587 (theoretical m/z = 572.2586), are presented in **Figure 5A and B**, respectively. This isotope cluster was absent in the RbIgG-IP from WT brain and in the Rb$\alpha K_V4.2$-IP from $K_V4.2^{-/-}$ brain as shown in the display of summed intensities in **Figure 5B**. The fourteen additional $K_V4.2$ peptides (as well as the peptides from the other $K_V4.2$ channel complex components) identified are indicated by the black vertical bar in the hierarchical cluster of the aligned peptide ion currents of the three IPs in **Figure 5C**. These analyses revealed that (except for the region indicated by the black vertical bar) the Rb$\alpha K_V4.2$-IP from WT brain was more similar to the Rb$\alpha K_V4.2$-IP from $K_V4.2^{-/-}$ brain (compare lanes 1 and 2 in **Fig. 5C**) than to the RbIgG-IP from WT brain (**Fig. 5C, lane 3**). These results suggest that the majority of contaminating proteins reflect the presence of the (rabbit) polyclonal anti-$K_V4.2$ antibody used for the immunoprecipitations, and that the optimal control, therefore, would be the $K_V4.2^{-/-}$ brain samples.

Once the detergent and control conditions were optimized, another, more comprehensive, in-solution approach, called Multidimensional Protein Identification Technology (MudPIT),[29,30] was employed. In this strategy, tryptic peptides obtained from the in-solution digestion were separated on a two-dimensional liquid chromatography column directly in line with a mass spectrometer (2D-LC-MS/MS). Similar to the in-solution 1D-LC-MS/MS approach, the MudPIT analyses yielded greater numbers of peptides and greater amino acid sequence coverage for most of the proteins identified (**Table 3**). More importantly, however, the MudPIT analyses resulted in the identification of additional proteins (i.e., in addition to the previously identified K_V4 channel KChIP/DPPx accessory subunits) that were observed only in the Rb$\alpha K_V4.2$-IP from WT mouse brain. For example, four unique (and six total) peptides corresponding to the voltage-gated K^+ (K_V) channel regulatory subunit, $K_V\beta1$, were identified in the Rb$\alpha K_V4.2$-IP from WT brain, but not in the two control IPs (**Table 3**). In addition, the $\alpha6$ subunit (Gabra-6) of the gamma-amino butyric acid (GABA-A) receptor, the G protein-coupled receptor 158 (Gpr158) and the $\beta1$ subunit (Prkcb1) of protein kinase C were also identified specifically in the Rb$\alpha K_V4.2$-IP from WT mouse brain (**Table 3**). These observations suggest the interesting possibility that these additional proteins are components of brain macromolecular K_V4 channel complexes and that they play roles in regulating the expression and/or the functioning of $K_V4.2$-encoded I_A channels.

In **Figure 6A**, the amino acid sequence coverages obtained for the $K_V4.2$ protein using the three different (in-gel and in-solution 1D-LC-MS/MS, and MudPIT) approaches are illustrated. When the peptides detected using the three different approaches are compiled (**Fig. 6A**), the overall amino acid sequence coverage for the $K_V4.2$ protein is calculated at 28%. Although this sequence coverage is quite good, it is of interest to note that nearly all of these peptides identified are located in the C- and N-termini of the $K_V4.2$ protein (**Fig. 6B**). One peptide in the intracellular S4-S5 loop was also detected. No peptides in the transmembrane domains of $K_V4.2$, however, were identified, likely reflecting the hydrophobic nature of the transmembrane domains.

Discussion

The results of the analyses presented here demonstrate that the immunoprecipitation approach for purifying $K_V4.2$-encoded I_A channel complexes from mouse brain works quite well, and, in addition, that it is possible to identify the components of these channel complexes by mass spectrometry. The use of the different in-gel and in-solution approaches in the experiments here allowed direct comparison of our ability to identify the protein components of brain $K_V4.2$ channel complexes. The results of these analyses clearly demonstrate the usefulness of the methodologies developed and exploited here and suggest that these approaches could, in theory, be applied to the analyses of other native ion channel complexes.

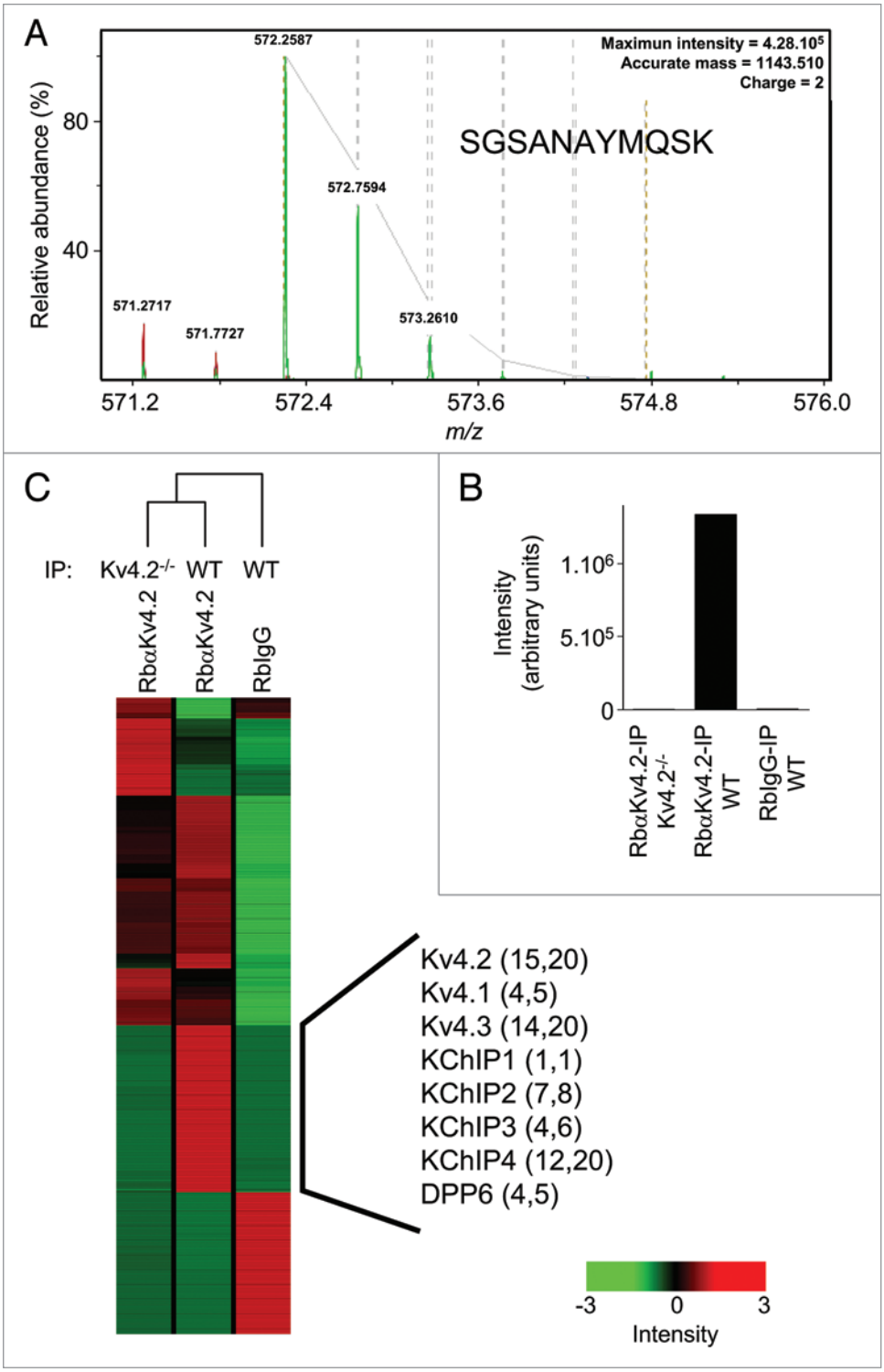

Figure 5. Quantification of peptides using high resolution, label-free 1D-LC-MS/MS. (A) Isotope cluster of a $K_V4.2$ peptide detected by 1D-LC-MS/MS analysis in the Rb$\alpha K_V4.2$-IP from WT brain. The peptide sequence (SGSANAYMQSK) was deduced from the tandem MS data given in Supplemental Table 2. (B) Summed intensities from the selected ion chromatograms at *m/z* = 572.2587 in the three IPs (RbIgG-IP from WT brain, Rb$\alpha K_V4.2$-IP from WT brain and Rb$\alpha K_V4.2$-IP from $K_V4.2^{-/-}$ brain) are illustrated. (C) Unsupervised partial hierarchical cluster of the summed peptide intensities from the three IPs. The aligned peptides in the Rb$\alpha K_V4.2$-IP from WT brain indicated by the black vertical line showed significant ($p < 0.001$) differences in summed intensities in the Rb$\alpha K_V4.2$-IP from WT brain compared with the Rb$\alpha K_V4.2$-IP from $K_V4.2^{-/-}$ brain. Identified proteins are listed, and the numbers of unique and total peptides for each are indicated in parentheses. Each colored box in the cluster map represents the relative abundance of each of the identified peptides, with a continuum of relative abundance levels from dark green (lowest) to bright red (highest). As evident on the map, the Rb$\alpha K_V4.2$-IP from WT brain is quite similar to the Rb$\alpha K_V4.2$-IP from $K_V4.2^{-/-}$ brain than to the RbIgG-IP from WT brain (except the region indicated by the black vertical line), illustrating the usefulness of the $K_V4.2^{-/-}$ brain samples in these analyses (see text).

The in-gel approach. In combination with standard western blots, the in-gel approach used here was critical in allowing optimization of each of the immunoprecipitation steps, maximizing the yield and the purity of isolated $K_V4.2$ channel complexes, as well as determining the conditions to preserve protein-protein interactions between the complex components. The immediate objectives of the initial optimization steps were to visualize a gel band corresponding to the $K_V4.2$ protein and to maximize the amount of the $K_V4.2$ protein obtained. In-gel visualization based on molecular weight (and subsequent mass spectrometric identification) of the previously described K_V4 accessory subunits, the KChIPx[13,14] and the DPPx[11,12,14] proteins, was also possible by direct comparison with the two control IPs. One critical component of the optimization procedures completed here involved comparison of detergent conditions with the goal of maximizing the amounts of the $K_V4.x$ proteins obtained and the relative amounts of co-immunoprecipitated KChIPx and DPPx proteins. Interestingly, these experiments also revealed that the interactions between the K_V4 α subunit and the DPPx and KChIPx proteins have different sensitivities to the detergents used in the solubilizations. These observations are consistent with the results of previous studies,[33,34] suggesting that distinct biochemical and/or structural constraints underlie $K_V4.2$ protein interactions with the accessory DPPx and KChIPx proteins.

Table 3. Proteins identified in immunoprecipitated brain $K_V4.2$ channel complexes using MudPIT[1]

Protein	Numbers of peptides: unique (total)	% Amino acid sequence coverage
$K_V4.2$	8 (17)	14%
$K_V4.1$	3 (4)	8%
$K_V4.3$	8 (19)	15%
KChIP2	2 (2)	10%
KChIP3	4 (10)	13%
KChIP4	8 (12)	38%
DPP6	33 (140)	32%
DPP10	18 (40)	24%
$K_V\beta1$	4 (6)	11%
Gabra-6	1 (4)	3%
Gpr158	5 (8)	5%
Prkcβ1	3 (7)	8%

[1]The numbers of unique peptides, as well as the total numbers of peptides and the percent (%) amino acid sequence coverage, for each protein are presented. Mascot protein and peptide ion scores were greater than 30, and Scaffold protein probability scores were 100% (see Suppl. Table 3). None of the proteins listed were identified in the control immunoprecipitations.

The use of the in-gel approach also allowed determination and optimization of the control IP conditions. As illustrated here, although the immunoprecipitated samples were enriched in $K_V4.2$ (and several other K_V4 accessory proteins), contaminating proteins were numerous. The direct visualization and comparison of experimental and control IPs on the gels (and on the subsequent mass spectrometric analyses) revealed that most of the contaminating proteins reflect the anti-$K_V4.2$ antibody used for the immunoprecipitation. Therefore, before undertaking any more sensitive and comprehensive mass spectrometric analyses, like the MudPIT analyses, it was important to identify the best antibody for immunoprecipitations (data not shown). The use of brains from the $K_V4.2^{-/-}$ animals[10] has also proven to be a very useful control in these studies as the same antibody-beads could be used in both experimental and control IPs. If targeted deletion animals are not available, the choice of the non-specific control antibody would clearly become an important point to consider.

Although useful for the reasons just discussed, the in-gel approach has substantial limitations. As is evident in the data presented, for example, there are many contaminating proteins in the immunoprecipitated samples, making direct comparison of experimental and control IPs difficult except for the most abundant proteins. In other words, specific accessory/regulatory proteins in the channel complexes could be masked by more abundant contaminating proteins and, therefore, be missed. Another limitation is sensitivity: lower abundant proteins are simply not visible on the gels, and as a consequence, would not be analyzed further. This complication could reflect the fact that these are low abundance proteins or, alternatively, that they are proteins with lower affinity interactions (with the targeted $K_V4.2$ protein). Finally, it is also important to note, as described in previous studies, that some proteins, and particularly transmembrane proteins,[35] do not stain well in gel, which will ultimately result in excluding these proteins from mass spectrometric analyses.

The in-solution approaches. In the in-solution approaches, the entire immunoprecipitates were digested and sequenced by 1D- or 2D-LC-MS/MS in efforts to identify proteins that are: low abundance, do not stain well in gels, or are masked by the more abundant proteins in the gels. Similar to the in-gel approach, the in-solution (1D- and 2D-LC-MS/MS) approaches allowed the identification of the $K_V4.x$, the KChIPx and the DPPx proteins. Importantly, the numbers of (unique and total) peptides detected, as well as the amino acid sequence coverages obtained for each of these proteins, were, in most cases, greater than those obtained with the targeted in-gel approach. This technical advantage of the in-solution digestion (over the in-gel digestion) approach is related to an inefficient extraction of tryptic peptides out of the gel matrix.[36] In future studies, the use of novel surfactant molecules, developed to optimize protein solubilization, in-gel trypsin digestion and peptide recovery from the gel might help to minimize this technical limitation.[37]

The MudPIT[29,30] approach enabled the identification of additional and novel brain $K_V4.2$ channel complex components. In this technology, the chromatographic separation is longer and takes place in two dimensions, allowing the separation and the sequencing of greater numbers of peptides and the identification of more proteins. The specific identification of several more proteins in the Rb$\alpha K_V4.2$-IP from WT brain (but not in the two control IPs) suggests the interesting possibility that these proteins correspond to specific accessory subunits and/or regulators of native brain $K_V4.2$ channels. One of these novel proteins was the K_V channel accessory subunit, $K_V\beta1$. Although the $K_V\beta$ subunits were initially suggested to be specific accessory subunits of K_V1 α subunit-encoded channels,[4] the results here suggest that $K_V\beta1$ might also function as a component/regulator of brain $K_V4.2$ channels. This finding is particularly interesting in light of previous studies suggesting possible physical and functional interactions between K_V4 and $K_V\beta$ subunits.[38,39] The identifications of the $\alpha6$ subunit (Gabra-6) of the gamma-aminobutyric acid (GABA-A) receptor as well as the G protein-coupled receptor 158 (Gpr158), which has been suggested to be a member of the glutamate G-protein coupled receptor subfamily,[40] in $K_V4.2$ channel complexes are particularly interesting observations in light of previous suggestions that $K_V4.2$-encoded I_A channels are localized at or near synapses and that these channels play a role in the regulation of synaptic responses and synaptic plasticity.[17-20] In addition, the identification of the $\beta1$ subunit (Prkcb1) of protein kinase C is potentially relevant to the phosphorylation of $K_V4.2$ channel subunits.[41] Additional biochemical and functional analyses aimed at investigating the regulation of $K_V4.2$ channels by these newly identified interacting proteins are warranted.

Advantages and limitations of proteomic approaches. The proteomic approaches presented here offer several advantages over more classical methods for identifying interacting proteins, such as two-hybrid screening in bacteria or yeast, or GST-pull-downs. In these more classical methods, the protein-protein interactions studied are not those observed in intact cells or in the native conformational states of the proteins. Furthermore,

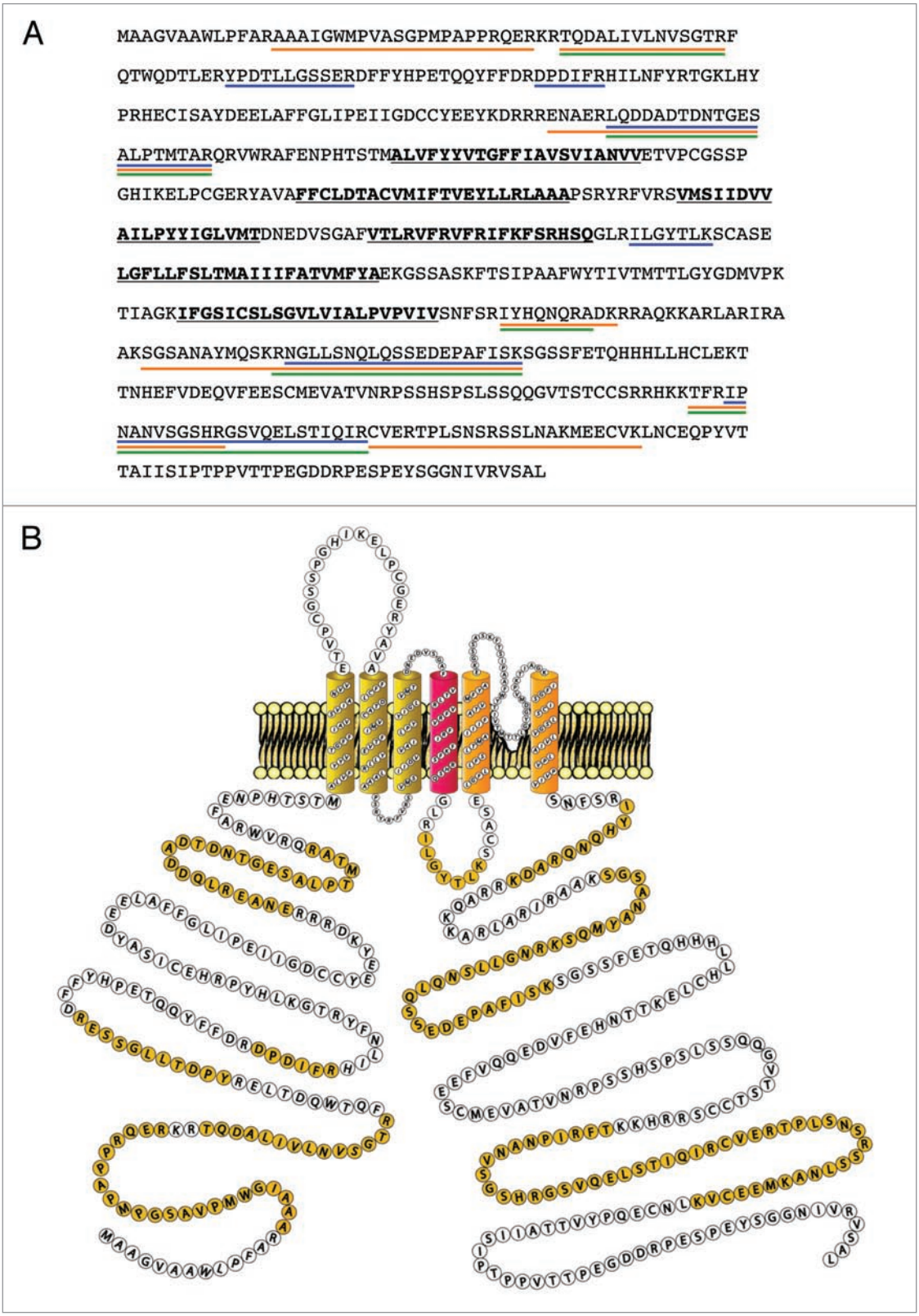

Figure 6. Amino acid sequence coverage of the K_V4.2 protein using the three proteomic approaches described. (A) K_V4.2 tryptic peptides detected using in-gel 1D-LC-MS/MS, in-solution 1D-LC-MS/MS, and MudPIT approaches are underlined in blue, orange and green, respectively. Transmembrane domains are in bold and underlined in black. (B) Schematic representation of mouse K_V4.2 channel protein along with MS/MS-detected peptides (highlighted in yellow).

in many of the classical studies, interactions between proteins were identified using peptide fragments, rather than full-length proteins. The use of native tissues is one of the main advantages of the proteomic strategies developed here over these more classical methods. Nevertheless, the possibility that non-physiological protein interactions take place during the lysis and immunoaffinity isolation experiments, rather than endogenously, cannot be excluded. To circumvent (or minimize) this possible complication, protein-protein cross-linking before protein solubilization, coupled with stringent immunoprecipitation conditions, could be employed.[42]

Finally, it is important to emphasize that proteomic data provide no direct information regarding protein function, and that it is necessary, therefore, to validate the functional roles of newly identified interacting proteins, particularly in native cells, using alternative experimental approaches.

Improvements in proteomic analyses. As illustrated in this study, although the immunoprecipitated samples were enriched in the channel protein complexes, the contaminating proteins were still numerous. Contaminating proteins are problematic for two reasons. First, they prevent the visualization of less abundant proteins on gels. But, more importantly, in the in-solution approach, they prevent the sequencing of the less abundant peptides. This well-recognized phenomenon in mass spectrometric analyses is called undersampling.[43] It is related to the fact that in any conventional (data-dependent) mass spectrometry-based proteomic experiment, only a small subset of the peptides present, the most abundant ones, are selected for fragmentation and sequencing. As it is difficult, if not impossible, to get rid of these abundant and contaminating proteins biochemically, one alternative is to target, during mass spectrometric experiments, peptides that are differentially present in the experimental, as compared with the control, IPs (rather than targeting the most abundant peptides in each IP).[32,44] Although not presently available, this new approach, called data-driven analysis, should allow more sensitive mass spectrometric protein identifications to be completed.

Materials and Methods

Animals were handled in accordance with the Guide for the Care and Use of Laboratory Animals (NIH).

Immunoprecipitation of brain $K_V4.2$ channel complexes. Flash-frozen brains from adult wild type (WT) mice or from mice ($K_V4.2^{-/-}$)[10] harboring a targeted disruption in the gene (*KCND2*) encoding $K_V4.2$ were homogenized in ice-cold lysis buffer containing (in mM) HEPES 20 (pH 7.4), potassium acetate 110 (pH 7.4), $MgCl_2$ 1, NaCl 150, with 0.1 μM $CaCl_2$, complete mini EDTA-free protease inhibitor cocktail tablet (Roche), 1 mM Pefabloc (Sigma), 1 ug/ml pepstatin A (Calbiochem), 1X Halt phosphatase inhibitor cocktail (Pierce) and one the following detergents/detergent conditions: 1% Triton X-100, 0.5% CHAPS or RIPA buffer (containing 0.5% sodium deoxycholate, 1% Triton X-100 and 0.1% Tween 20). After 15-min rotation at 4°C, 40 mg of the soluble protein fractions from the WT and $K_V4.2^{-/-}$ brains were used for immunoprecipitations (IP) with 100 μg of an anti-$K_V4.2$ rabbit polyclonal antibody (Rb$\alpha K_V4.2$, Chemicon). Parallel control experiments were completed using the same amount (100 μg) of non-specific rabbit immunoglobulin G (RbIgG, Santa Cruz Biotechnology, Inc.). Prior to immunoprecipitations, antibodies were cross-linked to 200 μl *of* protein A-magnetic beads (Invitrogen) using 20 mM dimethyl pimelimidate (Pierce).[25] Protein samples and antibody-coupled beads were mixed for two hours at 4°C. Magnetic beads were then collected, washed rapidly four times with ice-cold lysis buffer, and isolated protein complexes were eluted from the beads in 1X Sodium Dodecyl Sulfate (SDS) sample buffer (for the in-gel approach), or in 2% Rapigest[26] (Waters), 100 mM Tris (pH 8.5) (for the in-solution approaches), at 60°C for 5 min.

Endoprotease digestions in polyacrylamide gels and in solution. For the in-gel experiments, proteins were separated on one-dimensional polyacrylamide gels (1D-gels) after treatment with 100 mM dithiothreitol (DTT). The gels were fixed, stained with SYPRO Ruby (Invitrogen) and scanned. Using previously described methods,[27] individual bands were excised, and proteins were reduced, alkylated and digested with 0.2 μg/μl sequencing grade modified trypsin (Sigma). The resulting tryptic peptides were extracted from the gel band, desalted using C_{18} ZipTip (Waters), and reconstituted in aqueous 1% acetonitrile/0.1% formic acid for one-dimensional liquid chromatography-tandem mass spectrometric experiments (1D-LC-MS/MS).

Peptides were also prepared by endoprotease digestion of proteins[28] that were eluted from antibody-beads with Rapigest[26] (2%). The proteins were precipitated using the 2D protein clean up kit (GE Healthcare). The resulting pellets were dissolved in 8 M urea, 100 mM Tris (pH 8.5), reduced with 5 mM TCEP (pH 8.0) for 30 min at room temperature, and alkylated with 10 mM iodoacetamide (BioRad) for 30 min at room temperature. Samples were then digested with 1 μg endoproteinase Lys-C (Roche) overnight at 37°C, and subsequently with 4 μg of trypsin (Sigma) overnight at 37°C. Peptides were acidified with formic acid, extracted with NuTip porous graphite carbon wedge tips (Glygen), and eluted with aqueous acetonitrile (60%) containing formic acid (0.1%). The extracted peptides were dried, dissolved in aqueous acetonitrile/formic acid (1%/1%), stored at -80°C and subsequently analyzed using 1D-LC-MS/MS.

1D-LC-MS/MS. The high resolution 1D-LC-MS/MS analysis of peptides from in situ gel, or in-solution, endoprotease digestion was performed using a hybrid linear quadrupole ion trap-Fourier transform-ion cyclotron resonance mass spectrometer (LTQ-FTICR-MS, Thermo-Fisher).[28] The nanoflow high performance liquid chromatography (Nano LC-1D, Eksigent) was interfaced to the LTQ-FTICR with a nanospray source (PicoView PV550, New Objective). Sample injection was performed with an autosampler (AS1, Eksigent). Reverse phase C_{18} columns (MagicC18, Michrom Bioresources) were self-packed (PicoFrit, 75 μm x 10 cm, New Objective) and used for gradient separation of peptides. Both the aqueous phase (LC-MS water, Riedel-de Haen) and organic phase (LC-MS acetonitrile, Riedel-de Haen) were modified with 0.1% formic acid (Sigma). Five or ten μL samples were loaded at 1 μL/min from a 10 μL loop. After an initial aqueous wash at 260 nL/min, the organic phase for the analytical gradient was increased at 0.6–1.2% per

minute up to 70% organic also at 260 nL/min. The nanospray source was operated between 1.8 and 2.3 kV with sheath gas and the spray was visually optimized ~20% organic flow at 260 nL/min. The capillary temperature was 240°C. Tandem spectra were acquired in data-dependent mode. Full MS scans were acquired at 100,000 resolving power (*m/z* 421.75) with a target value of 1,000,000. The ion trap MS^n target was 20,000. For data-dependent scans, the six most intense ions were selected for wideband collisional activation and detection in the ion trap (parent threshold = 1000; isolation width = 2.0 Da; normalized collision energy = 35; activation Q = 0.250; activation time = 30 ms). Dynamic exclusion was employed to expand selection.

MudPIT. For the Multidimensional Protein Identification Technology[29,30] experiments, immunoprecipitated protein samples were eluted from the beads, reduced, alkylated, trypsinized and analyzed as described previously.[31] In brief, a fritless, microcapillary (100 μm-inner diameter) column was packed sequentially with the following: 9 cm of 5 μm C_{18} reverse-phase (Synergi 4 μ Hydro RP80a, Phenomenex), 3 cm of 5 μm strong cation exchange (Partisphere SCX, Whatman) and 2 cm of C_{18} reverse-phase packing material. The trypsin-digested samples were loaded directly onto the triphasic column equilibrated in 0.1% formic acid, 2% acetonitrile, which was then placed in line with a LTQ linear ion trap mass spectrometer (Thermo, Inc.). An automated six-cycle multidimensional chromatographic separation was performed using buffer A (0.1% formic acid, 5% acetonitrile), buffer B (0.1% formic acid, 80% acetonitrile) and buffer C (0.1% formic acid, 5% acetonitrile, 500 mM ammonium acetate) at a flow rate of 300 nL/min. The first cycle was a 20-min isocratic flow of buffer B. Cycles 2–6 consisted of 3 min of buffer A, 2 min of 15–100% buffer C, 5 min of buffer A, followed by a 60-min linear gradient to 60% buffer B. In cycles 2–6, the percent of buffer C was increased gradually (from 15, 30, 50, 70 to 100%) in each cycle. During the linear gradient, eluting peptides were analyzed by one full MS scan (200–2,000 *m/z*), followed by five MS/MS scans on the five most abundant ions detected in the full MS scan while operating under dynamic exclusion.

Data analyses. The MS1 and MS2 data from the LTQ-FTICR mass spectrometer were acquired in the profile mode. To perform quantitative label-free analysis, the MS1 LC-MS data from separate LC analyses of control and experimental immunoprecipitates were aligned and normalized using the Rosetta Elucidator software (version 3.2, Rosetta Elucidator™, Rosetta Biosoftware, Seattle, WA).[32] The "raw" files were imported for feature retention time alignment, definition and volume determination within the selected LC-MS time window. The "PeakTeller" algorithm in the software performed background subtraction and smoothing in both the retention time and *m/z* dimensions using scores of 0.5 and 0.5, respectively. The "adaptive alignment" option was selected and the following additional parameters were used during the alignment process: instrument mass accuracy = 10 ppm, "Expected retention time shift" = 2 min and "Noise removal strength" for retention time and *m/z* were both set to 1 for both. The peak width time was set at >0.1 min. Intensity scaling was based on the mean intensities of all quality features (as defined above) and was performed after a 10% outlier trim to correct for variations in the total ion current between individual LC-MS analyses.

For analysis of the MS2 data from the LTQ-FTICR and the LTQ mass spectrometers, "raw" files were processed using MASCOT Distiller (Matrix Science, version 2.1) with the following settings: (1) MS processing: 200 data points per Da; no aggregation method; maximum charge state = +5; minimum number of peaks = 1; (2) MS/MS processing: 200 data points per Da; time domain aggregation method enabled; minimum number of peaks = 10; precursor charge and *m/z*, "try to re-determine from the survey scan (tolerance = 2.5 Da)"; charge defaults = +2/+3; maximum charge state = +2; (3) Time domain parameters: minimum precursor mass = 700; maximum precursor mass = 16,000; precursor *m/z* tolerance for grouping = 0.1; maximum number of intermediate scans = 5; minimum number of scans in a group = 1. Peak Picking: maximum iterations = 500; correlation threshold = 0.90; minimum signal-to-noise = 3; minimum peak *m/z* = 50; maximum peak *m/z* = 100,000; minimum peak width = 0.001; maximum peak width = 2; and expected peak width = 0.01. The files from the MASCOT DISTILLER output (mgf) for each individual LC-MS analysis were concatenated and searched against the Uniprot-mouse database (downloaded May, 2008). Peptide identifications obtained using the LTQ-FTICR were done using MASCOT, version 2.2.04 with the following parameters: Enzyme, trypsin; MS tolerance = 10 ppm, MS/MS tolerance = 0.8 Da with a fixed carbamidomethylation modification of the Cys residues and the following variable modifications: Met, oxidation; Pyro-glu (N-term) and Deamidation (Gln and Asn residues); Maximum Missed Cleavages = 1; and 1+, 2+ and 3+ charge states. Data from each MudPIT fraction were analyzed individually using a mass tolerance of ± 0.4 Da for both parent and fragment ions, and MASCOT protein scores for each protein were calculated by adding the MASCOT ion scores (greater than 30) of individual peptides. MASCOT-analyzed data were then analyzed using the Scaffold software (Proteome Software, Portland OR). Only protein identifications for which MASCOT protein and peptide ion scores were greater than 30, and Scaffold protein scores were 100%, were considered as true positives. Mass spectrometric data sets have been deposited into the Tranche data repository, and are available in the publicly accessible format mzXML using the following link: https://proteomecommons.org/tranche/.

Antibodies and western blot analyses. The brain $K_V4.2$ protein was detected using an anti-$K_V4.2$ mouse monoclonal antibody (m$\alpha K_V4.2$, K57/1), developed by and obtained from UC Davis/NIH NeuroMab Facility (supported by NIH grant U24NS050606 and maintained by the University of California, Davis, CA 95616). Bound primary antibodies were detected using horseradish peroxidase-conjugated goat anti-mouse secondary antibodies (Pierce). Protein signals were visualized using the SuperSignal West Dura Extended Duration substrate (Pierce).

Acknowledgements

The financial support provided by the Washington University—Pfizer Biomedical Research Program (to Jeanne M. Nerbonne), the National Institutes of Health (R01-HL034161 to Jeanne M.

Nerbonne, R01-GM064779 to Andrew J. Link), the National Center for Research Resources (NIH P41RR000954), the NIH Neuroscience Blueprint Center Core Grant (P30-NS057105), the W.M. Keck Foundation, and the Heartland Affiliate of the American Heart Association (Postdoctoral Fellowship to Céline Marionneau) is gratefully acknowledged.

Note

Supplementary materials can be found at: www.landesbioscience.com/supplement/MarionneauCHAN3-4-Sup.pdf

References

1. Hoffman DA, Magee JC, Colbert CM, Johnston D. K^+ channel regulation of signal propagation in dendrites of hippocampal pyramidal neurons. Nature 1997; 387:869-75.
2. Jerng HH, Pfaffinger PJ, Covarrubias M. Molecular physiology and modulation of somatodendritic A-type potassium channels. Mol Cell Neurosci 2004; 27:343-69.
3. Birnbaum SG, Varga AW, Yuan LL, Anderson AE, Sweatt JD, Schrader LA. Structure and function of K_V4-family transient potassium channels. Physiol Rev 2004; 84:803-33.
4. Yu FH, Yarov-Yarovoy V, Gutman GA, Catterall WA. Overview of molecular relationships in the voltage-gated ion channel superfamily. Pharmacol Rev 2005; 57:387-95.
5. Mohler PJ, Wehrens XH. Mechanisms of human arrhythmia syndromes: abnormal cardiac macromolecular interactions. Physiology (Bethesda) 2007; 22:342-50.
6. Nerbonne JM, Kass RS. Molecular physiology of cardiac repolarization. Physiol Rev 2005; 85:1205-53.
7. Kim J, Wei DS, Hoffman DA. K_V4 potassium channel subunits control action potential repolarization and frequency-dependent broadening in rat hippocampal CA1 pyramidal neurones. J Physiol 2005; 569:41-57.
8. Yuan W, Burkhalter A, Nerbonne JM. Functional role of the fast transient outward K^+ current I_A in pyramidal neurons in (rat) primary visual cortex. J Neurosci 2005; 25:9185-94.
9. Malin SA, Nerbonne JM. Elimination of the fast transient in superior cervical ganglion neurons with expression of $K_V4.2W362F$: molecular dissection of I_A. J Neurosci 2000; 20:5191-9.
10. Nerbonne JM, Gerber BR, Norris A, Burkhalter A. Electrical remodelling maintains firing properties in cortical pyramidal neurons lacking KCND2-encoded A-type K^+ currents. J Physiol 2008; 586:1565-79.
11. Nadal MS, Ozaita A, Amarillo Y, Vega-Saenz de Miera E, Ma Y, Mo W, et al. The CD26-related dipeptidyl aminopeptidase-like protein DPPX is a critical component of neuronal A-type K^+ channels. Neuron 2003; 37:449-61.
12. Zagha E, Ozaita A, Chang SY, Nadal MS, Lin U, Saganich MJ, et al. DPP10 modulates K_V4-mediated A-type potassium channels. J Biol Chem 2005; 280:18853-61.
13. Rhodes KJ, Carroll KI, Sung MA, Doliveira LC, Monaghan MM, Burke SL, et al. KChIPs and K_V4 alpha subunits as integral components of A-type potassium channels in mammalian brain. J Neurosci 2004; 24:7903-15.
14. Jerng HH, Kunjilwar K, Pfaffinger PJ. Multiprotein assembly of $K_V4.2$, KChIP3 and DPP10 produces ternary channel complexes with ISA-like properties. J Physiol 2005; 568:767-88.
15. Maffie J, Rudy B. Weighing the evidence for a ternary protein complex mediating A-type K^+ currents in neurons. J Physiol 2008; 586:5609-23.
16. Kim J, Nadal MS, Clemens AM, Baron M, Jung SC, Misumi Y, et al. K_V4 accessory protein DPPX (DPP6) is a critical regulator of membrane excitability in hippocampal CA1 pyramidal neurons. J Neurophysiol 2008; 100:1835-47.
17. Burkhalter A, Gonchar Y, Mellor RL, Nerbonne JM. Differential expression of I(A) channel subunits $K_V4.2$ and $K_V4.3$ in mouse visual cortical neurons and synapses. J Neurosci 2006; 26:12274-82.
18. Jung SC, Kim J, Hoffman DA. Rapid, bidirectional remodeling of synaptic NMDA receptor subunit composition by A-type K^+ channel activity in hippocampal CA1 pyramidal neurons. Neuron 2008; 60:657-71.
19. Andrasfalvy BK, Makara JK, Johnston D, Magee JC. Altered synaptic and non-synaptic properties of CA1 pyramidal neurons in $K_V4.2$ knockout mice. J Physiol 2008; 586:3881-92.
20. Kim J, Hoffman DA. Potassium channels: newly found players in synaptic plasticity. Neuroscientist 2008; 14:276-86.
21. Sandoz G, Lesage F. Protein complex analysis of native brain potassium channels by proteomics. Methods Mol Biol 2008; 491:113-23.
22. Yan J, Olsen JV, Park KS, Li W, Bildl W, Schulte U, et al. Profiling the phospho-status of the BKCa channel alpha subunit in rat brain reveals unexpected patterns and complexity. Mol Cell Proteomics 2008; 7:2188-98.
23. Park KS, Mohapatra DP, Misonou H, Trimmer JS. Graded regulation of the $K_V2.1$ potassium channel by variable phosphorylation. Science 2006; 313:976-9.
24. Yang JW, Vacher H, Park KS, Clark E, Trimmer JS. Trafficking-dependent phosphorylation of $K_V1.2$ regulates voltage-gated potassium channel cell surface expression. Proc Natl Acad Sci USA 2007; 104:20055-60.
25. Schneider C, Newman RA, Sutherland DR, Asser U, Greaves MF. A one-step purification of membrane proteins using a high efficiency immunomatrix. J Biol Chem 1982; 257:10766-9.
26. Yu YQ, Gilar M, Gebler JC. A complete peptide mapping of membrane proteins: a novel surfactant aiding the enzymatic digestion of bacteriorhodopsin. Rapid Commun Mass Spectrom 2004; 18:711-5.
27. Hu Y, Malone JP, Fagan AM, Townsend RR, Holtzman DM. Comparative proteomic analysis of intra- and interindividual variation in human cerebrospinal fluid. Mol Cell Proteomics 2005; 4:2000-9.
28. King JB, Gross J, Lovly CM, Piwnica-Worms H, Townsend RR. Identification of protein phosphorylation sites within Ser/Thr-rich cluster domains using site-directed mutagenesis and hybrid linear quadrupole ion trap Fourier transform ion cyclotron resonance mass spectrometry. Rapid Commun Mass Spectrom 2007; 21:3443-51.
29. Link AJ, Eng J, Schieltz DM, Carmack E, Mize GJ, Morris DR, et al. Direct analysis of protein complexes using mass spectrometry. Nat Biotechnol 1999; 17:676-82.
30. Washburn MP, Wolters D, Yates JR, 3rd. Large-scale analysis of the yeast proteome by multidimensional protein identification technology. Nat Biotechnol 2001; 19:242-7.
31. Arnett DR, Jennings JL, Tabb DL, Link AJ, Weil PA. A proteomics analysis of yeast Mot1p protein-protein associations: insights into mechanism. Mol Cell Proteomics 2008; 7:2090-106.
32. Neubert H, Bonnert TP, Rumpel K, Hunt BT, Henle ES, James IT. Label-free detection of differential protein expression by LC/MALDI mass spectrometry. J Proteome Res 2008; 7:2270-9.
33. Seikel E, Trimmer JS. Convergent modulation of $K_V4.2$ channel alpha subunits by structurally distinct DPPX and KChIP auxiliary subunits. Biochemistry 2009; 48:5721-30.
34. Shibata R, Misonou H, Campomanes CR, Anderson AE, Schrader LA, Doliveira LC, et al. A fundamental role for KChIPs in determining the molecular properties and trafficking of $K_V4.2$ potassium channels. J Biol Chem 2003; 278:36445-54.
35. Hart C, Schulenberg B, Patton WF. Selective proteome-wide detection of hydrophobic integral membrane proteins using a novel fluorescence-based staining technology. Electrophoresis 2004; 25:2486-93.
36. Meng W, Zhang H, Guo T, Pandey C, Zhu Y, Kon OL, Sze SK. One-Step Procedure for Peptide Extraction from In-Gel Digestion Sample for Mass Spectrometric Analysis. Anal Chem 2008.
37. Saveliev S, Simpson D, Daily W, Woodroofe C, Klaubert D, Sabat G, et al. Improve protein analysis with the new, mass spectrometry-compatible ProteasMAX surfactant. Promega Notes 2008; 99:3-7.
38. Yang EK, Alvira MR, Levitan ES, Takimoto K. $K_V$beta subunits increase expression of $K_V4.3$ channels by interacting with their C termini. J Biol Chem 2001; 276:4839-44.
39. Aimond F, Kwak SP, Rhodes KJ, Nerbonne JM. Accessory $K_V$beta1 subunits differentially modulate the functional expression of voltage-gated K^+ channels in mouse ventricular myocytes. Circ Res 2005; 96:451-8.
40. Bjarnadottir TK, Fredriksson R, Schioth HB. The gene repertoire and the common evolutionary history of glutamate, pheromone (V2R), taste(1) and other related G protein-coupled receptors. Gene 2005; 362:70-84.
41. Schrader LA, Ren Y, Cheng F, Bui D, Sweatt JD, Anderson AE. $K_V4.2$ is a locus for PKC and ERK/MAPK cross-talk. Biochem J 2009; 417:705-15.
42. Schmitt-Ulms G, Hansen K, Liu J, Cowdrey C, Yang J, DeArmond SJ, et al. Time-controlled transcardiac perfusion cross-linking for the study of protein interactions in complex tissues. Nat Biotechnol 2004; 22:724-31.
43. Garza S, Moini M. Analysis of complex protein mixtures with improved sequence coverage using (CE-MS/MS)n. Anal Chem 2006; 78:7309-16.
44. America AH, Cordewener JH. Comparative LC-MS: a landscape of peaks and valleys. Proteomics 2008; 8:731-49.